Impaired insulin secretion and glucose intolerance in synaptotagmin-7 null mutant mice

Natalia Gustavsson[†], Ye Lao[‡], Anton Maximov[‡], Jen-Chieh Chuang[§], Elena Kostromina[†], Joyce J. Repa[§], Cai Li[§¶], George K. Radda[†], Thomas C. Südhof[‡‖], and Weiping Han[†‡‖††]

[†]Laboratory of Metabolic Medicine, Singapore Bioimaging Consortium, Agency for Science, Technology, and Research (A*STAR), Singapore 138667; [‡]Center for Basic Neuroscience, Howard Hughes Medical Institute and [§]Department of Physiology, University of Texas Southwestern Medical Center, Dallas, TX 75235; [¶]Merck Research Laboratories, Rahway, NJ 07065; and [††]Department of Biochemistry, Yong Loo Lin School of Medicine, National University of Singapore, Singapore 117597

Communicated by Britton Chance, University of Pennsylvania School of Medicine, Philadelphia, PA, December 15, 2007 (received for review August 23, 2007)

Vertebrates express at least 15 different synaptotagmins with the same domain structure but diverse localizations and tissue distributions. Synaptotagmin-1,-2, and -9 act as calcium sensors for the fast phrase of neurotransmitter release, and synaptotagmin-12 acts as a calcium-independent modulator of release. The exact functions of the remaining 11 synaptotagmins, however, have not been established. By analogy to the role of synaptotagmin-1, -2, and -9 in neurotransmission, these other synaptotagmins may serve as Ca^{2+} transducers regulating other Ca^{2+}-dependent membrane processes, such as insulin secretion in pancreatic β-cells. Of these other synaptotagmins, synaptotagmin-7 is one of the most abundant and is present in pancreatic β-cells. To determine whether synaptotagmin-7 regulates Ca^{2+}-dependent insulin secretion, we analyzed synaptotagmin-7 null mutant mice for glucose tolerance and insulin release. Here, we show that synaptotagmin-7 is required for the maintenance of systemic glucose tolerance and glucose-stimulated insulin secretion. Mutant mice have normal insulin sensitivity, insulin production, islet architecture and ultrastructural organization, and metabolic and calcium responses but exhibit impaired glucose-induced insulin secretion, indicating a calcium-sensing defect during insulin-containing secretory granule exocytosis. Taken together, our findings show that synaptotagmin-7 functions as a positive regulator of insulin secretion and may serve as a calcium sensor controlling insulin secretion in pancreatic β cells.

calcium sensor | exocytosis | glucose tolerance | insulin sensitivity | NADH

The predominant form of diabetes, type 2 or non-insulin-dependent diabetes mellitus, develops as a result of insulin secretory dysfunction and peripheral insulin resistance (1). Secretory dysfunction in pancreatic β-cells (i.e., a reduction of stimulated insulin secretion) is thought to be caused by insufficient signal level secondary to impaired glucose metabolism and the resultant incomplete closure of the K_{ATP}-channels and/or deficiencies in the exocytotic mechanism itself (2, 3). Glucose-stimulated insulin secretion has a biphasic pattern, which consists of a 10- to 15-min rapid first phase and a less-prominent but sustained second phase (4). The first phase of insulin secretion requires a rapid and marked elevation of intracellular Ca^{2+} concentration ($[Ca^{2+}]_i$), whereas the second phase requires amplifying signals from glucose metabolism in addition to oscillatory $[Ca^{2+}]_i$ (3). Partial or complete loss of the first phase of glucose-induced insulin release is a characteristic deterioration in early stages of type 2 diabetes (4, 5). Defects of the second phase develop at a slower time course but become equally prominent as diabetes progresses (6). Although much progress has been made in understanding the role of insulin secretion in the pathogenesis of diabetes, the molecular mechanisms of normal β cell function, such as Ca^{2+} regulation of insulin release, are poorly understood.

Insulin release is a complex and highly regulated process. Under physiological conditions, an elevation of blood glucose triggers rapid uptake of glucose into pancreatic β-cells. Glucose metabolism in β-cells results in increased ATP/ADP ratio, which leads to K_{ATP} channel closure, membrane depolarization, and subsequent opening of voltage-gated Ca^{2+} channels and the rise in cytoplasmic Ca^{2+} concentration (7). It has been established that the $[Ca^{2+}]$ rise is the trigger for insulin-containing granule exocytosis, which is likely executed by SNARE complex (8). Besides the SNARE proteins, numerous proteins that may be involved in the regulation of insulin secretion have been identified (9), including several synaptotagmins (10–15), but the precise mechanisms by which calcium signal is transduced in pancreatic β-cells are not clear.

Studies using genetically modified animals have established that synaptotagmin-1, -2, and -9 are calcium sensors for the fast phase of neurotransmitter release (16–22). However, the slow component of neurotransmitter release remains in animals without these synaptotagmins (18). Furthermore, normal Ca^{2+}-stimulated secretion is still observed in PC12 cells lacking synaptotagmin-1 and -2 (23). These studies indicate that additional protein(s) must be responsible for Ca^{2+} sensing in these release processes in the absence of synaptotagmin-1, -2, and -9. Besides synaptotagmin-1, -2, and -9, 12 other synaptotagmins have been cloned (24, 25). All synaptotagmins share a common domain structure: a short N-terminal sequence followed by a transmembrane region, a linker sequence, and two C-terminal C_2-domains (26). Of these "other" synaptotagmins, synaptotagmin-7 is one of the most abundant with multiple splicing forms that are developmentally regulated and present in pancreatic β-cells (10, 24, 27). Furthermore, studies in permeabilized PC12 cells demonstrated that the C_2-domains of synaptotagmin-7 potently inhibited exocytosis, indicating a role of synaptotagmin-7 in regulating neuroendocrine secretion (27), although synaptotagmin-9 was suggested to act here instead of synaptotagmin-7 (28). The C_2-domains of synaptotagmin-7 have a 10- to 20-fold higher Ca^{2+} affinity than those of synaptotagmin-1 and -2 (29). Insulin secretion has been shown to have a wide range of Ca^{2+} sensitivities, responding to both high ($K_d \approx 20\ \mu M$) and low ($K_d \approx 1\ \mu M$) Ca^{2+} stimulations; thus indicating the presence of more than one Ca^{2+} sensor in β-cells (30). Synaptotagmin-7 binds to Ca^{2+} at micromolar levels and is localized to β-cells, supporting its role as a high-affinity Ca^{2+} sensor for insulin release.

Author contributions: J.J.R., C.L., G.K.R., T.C.S., and W.H. designed research; N.G., Y.L., A.M., J.-C.C., E.K., and W.H. performed research; N.G., Y.L., A.M., J.-C.C., E.K., and W.H. analyzed data; and N.G., T.C.S., and W.H. wrote the paper.

The authors declare no conflict of interest.

Freely available online through the PNAS open access option.

‖To whom correspondence may be addressed. E-mail: thomas.sudhof@utsouthwestern.edu or weiping_han@sbic.a-star.edu.sg.

This article contains supporting information online at www.pnas.org/cgi/content/full/0711700105/DC1.

To investigate whether synaptotagmin-7 regulates Ca^{2+}-dependent insulin secretion in β-cells *in vivo*, we studied synaptotagmin-7 mutant mice for their glucose tolerance and glucose-stimulated insulin release at the whole-animal-level and characterized isolated pancreatic islets on the cellular and ultrastructural levels. Here, we show that synaptotagmin-7 is required for the maintenance of systemic glucose tolerance and glucose-stimulated insulin secretion. Mutant mice exhibit normal insulin sensitivity and normal metabolic and calcium responses but impaired insulin release, which indicates a calcium sensing defect in these mice. Our findings suggest that synaptotagmin-7 functions as a positive regulator of insulin secretion and support that synaptotagmin-7 serves as a Ca^{2+} sensor in pancreatic β-cells.

Results

Synaptotagmin-7 Is Expressed in Insulin-Secreting Cells. Besides synaptotagmin-1, -2, and -9, several other synaptotagmins (synaptotagmin-3, -5, -6, -7, and -10) have Ca^{2+} binding affinities consistent with their potential role as Ca^{2+} sensors (29, 31, 32). To test whether a synaptotagmin-1/2 paradigm exists in pancreatic β-cells, i.e., other synaptotagmins function as Ca^{2+} sensors for insulin secretion, we first performed Western blot analysis on two insulin secreting cell lines (RIN and INS-1) and examined the expression of specific synaptotagmins. Consistent with previous reports, we found that several synaptotagmins, including synaptotagmin-7, were expressed in insulin secreting cells [supporting information (SI) Fig. 6] along with SNARE proteins (Syntaxin 1, Synaptobrevin 2, and SNAP-25) and α/β-SNAPs (SI Fig. 7). In contrast, synaptic vesicle-specific proteins, such as synaptophysin or synaptogyrin, were absent in these cells (SI Fig. 7). To examine the relative mRNA levels of all synaptotagmins, we performed qPCR analysis of samples from mouse islets and insulin- and glucagon-secreting cell lines. Synaptotagmin-7 transcript was present at high levels in islets and the glucagon-secreting cell line and at moderate levels in the two insulin-secreting cell lines tested (SI Fig. 8).

Expression of synaptotagmin-7 in insulin-secreting cells was further examined by immunofluorescence of mouse islet sections. The majority of insulin-reactive cells was located in the core of the islets, consistent with normal β cell distribution. Synaptotagmin-7 immunoreactivity was evident in insulin-containing β-cells from wild-type animals but absent from mutant mice (Fig. 1). In addition to β-cells, synaptotagmin-7 was also observed in non-insulin-reactive cells, including α-cells (Fig. 1 and T.C.S. and W.H., unpublished observation).

Synaptotagmin-7 Mutant Mice Exhibit Impaired Glucose Tolerance and Insulin Secretion *in Vivo*. To study the effects of synaptotagmin-7 deletion on systemic glucose homeostasis and insulin release *in vivo*, we performed i.p. glucose tolerance tests (IPGTT) on overnight-fasted synaptotagmin-7 mutant mice and their control littermates. An i.p. glucose challenge (2 g per kilogram of body weight) revealed an impaired glucose tolerance in male, but not female synaptotagmin-7 mutant mice. Females were less prone to insulin resistance and diabetes than males, possibly because of hormonal differences, which could render hormone-related phenotypes difficult to detect (33, 34). Therefore, we focused our studies on male mice. In IPGTT, mutant mice showed delayed glucose clearance with glucose levels higher than control mice at 15, 30, and 60 min after injection (Fig. 2*A*). Basal glucose levels were not different between fed or fasted mutant and control animals (Table 1). Insulin concentrations were also measured during the glucose tolerance test. Synaptotagmin-7 mutant mice showed lower insulin levels at 8 and 30 min after glucose injection (Fig. 2*B*). Insulin levels after overnight fasting were also lower in mutant mice but similar in fed animals (Table 1).

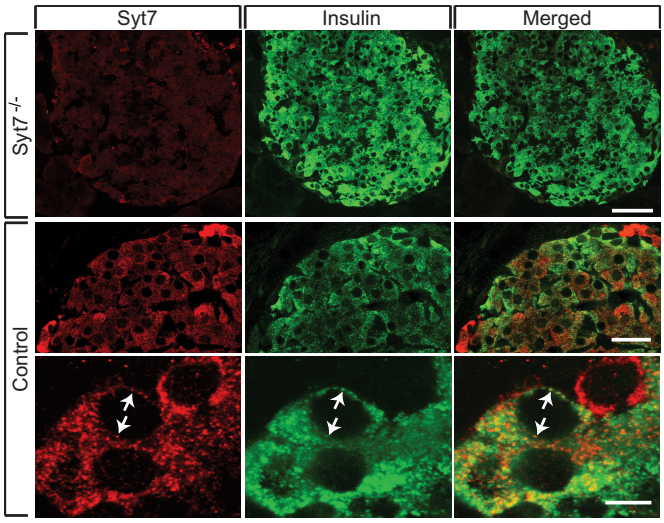

Fig. 1. Synaptotagmin-7 is present in mouse pancreatic β-cells. Twenty-micrometer pancreatic sections were first reacted with both a polyclonal rabbit antibody against synaptotagmin-7 (S757; Synaptic Systems) and a monoclonal guinea pig antibody against insulin, followed by fluorescence-conjugated secondary antibodies (Alexa Fluor 546 goat-anti-rabbit IgG and Alexa Fluor 488 Donkey-anti-Guinea Pig IgG). Representative images of such stained sections, taken on a Leica TCS2 confocal microscope, are shown. Synaptotagmin-7 (Syt7, red) was expressed in insulin-positive cells and shown to have high degree of overlap with insulin signals (green). Arrows indicate selected overlapping signals of insulin and synaptotagmin-7. For comparison, no apparent synaptotagmin-7 signal was detected in islet sections from synaptotagmin-7 mutant ($Syt7^{-/-}$) mouse. (Scale bars: 40, 20, and 5 μm for *Upper*, *Middle*, and *Bottom*, respectively.)

To test whether insulin sensitivity was normal in mutant mice, we performed insulin tolerance tests (ITT) on mutant and control mice after 2-h fasting. An i.p. insulin challenge (1 unit per kilogram of body weight) resulted in a more prominent blood glucose decrease in mutant than in control (Fig. 2*C*), indicating that synaptotagmin-7 mutant mice were not resistant to insulin, which otherwise could be responsible for the glucose intolerance.

Synaptotagmin-7 Mutant Mice Have Lower Body Weight and Fat Content than Controls. Body fat content, especially increased myocellular lipid content and elevated free fatty-acid concentrations, often have deleterious effects on glucose clearance (35), and high body fat correlates with a poor glucose tolerance (T.C.S. and W.H., unpublished observations). Therefore, we compared body weight, body fat, and body lean content of synaptotagmin-7 mutant and control mice. At 14 weeks, mutant mice had slightly lower body weight and body fat content than their controls of the same age group (Table 1). Body lean content was similar in mutant and control mice (Table 1).

Morphological and Ultrastructural Characteristics Are Normal in Synaptotagmin-7 Mutant Mouse Pancreatic Islets. We next examined whether the reduced insulin response was associated with changes in pancreatic islets. Histological analysis revealed no pathological signs in mutant mouse islets. Islets from mutant and control mice were of similar size and shape with smooth periphery (Fig. 3*A* and Table 1). No hemostasis, fibroblast proliferation, or excessive vascularization was observed in mutant mouse islets. Islet area, number of cells in single islets, and morphology of individual cells from histological sections were similar in mutant and control mice (Fig. 3*A* and Table 1).

To determine whether ultrastructural changes were responsible for the reduced insulin response in mutant mice, we performed EM analysis on pancreatic β-cells from both groups of

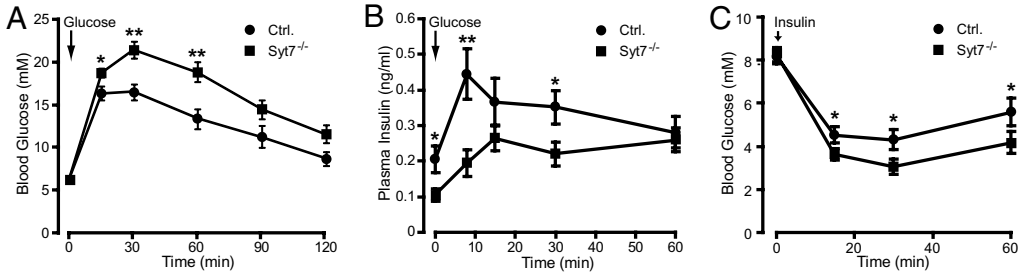

Fig. 2. Impaired glucose tolerance and insulin secretion, but normal insulin sensitivity in synaptotagmin-7 mutant mice. (*A*) An i.p. glucose tolerance test (IPGTT) was performed on overnight-fasted synaptotagmin-7 mutants and wild-type control mice. Blood glucose levels before and at 15, 30, 60, 90, and 120 min after glucose injection (2 mg per gram of body weight) were measured. Synaptotagmin-7 mutant (Syt7$^{-/-}$) mice (filled square, $n = 13$) exhibited glucose intolerance as evidenced by higher glucose concentration after injection and delayed clearance of glucose. *, $P < 0.02$, **, $P < 0.005$ vs. control (filled circle, $n = 17$). (*B*) Plasma insulin levels in control and synaptotagmin-7 mutant mice before and at 8, 15, 30, and 60 min of IPGTT were determined. Synaptotagmin-7 mutant mice showed insulin-secretory deficiency, especially in the first 15 min, upon glucose challenge. $n = 10$ for control (filled circle) and 11 for mutant (filled square). *, $P < 0.05$, **, $P < 0.005$. (*C*) Blood glucose levels were measured in 2-h-fasted control and mutant mice before and at 15, 30, and 60 min after injection of 1 unit/kg insulin. Synaptotagmin-7 mutant mice appeared to have higher insulin sensitivity than their wild-type control. *, $P < 0.03$, $n = 17$.

mice. β-cells were identified by their characteristic secretory granules containing an electron-dense core with a translucent halo. Islet β-cells from mutant and control mice contained numerous secretory granules, large nuclei with partly condensed chromatin, scattered lamellar rough endoplasmic reticulum, and often showed a well developed Golgi apparatus. The number of granules appeared similar in mutant and control mice (Fig. 3*B*)

Lower insulin production and insulin content may contribute to reduced insulin secretion and consequent glucose intolerance. We examined islet insulin content in isolated islets from mutant and control mice (Fig. 3*C*). Islet volume was measured first ($3.3 \pm 0.4 \times 10^{-3}$ mm^3 vs. $3.2 \pm 0.5 \times 10^{-3}$ mm^3, control vs. mutant, $n = 19$, NS) before the islets were lysed and insulin levels were measured by using ELISA. There was no difference in insulin content between mutant and control mice (Fig. 3*C*). Insulin mRNA levels were also similar in control and mutant animals as determined by qPCR from isolated islets (Fig. 3*D*). These results provide further evidence that insulin secretory dysfunction was not caused by defects in insulin production or islet architecture and organization.

NAD(P)H and Ca^{2+} Responses are Normal in Synaptotagmin-7 Mutant Mice. Combined redox signal from NADH and NADPH [NAD(P)H] in glucose-stimulated islets, a measure of mitochondrial and glycolytic function (36), was used to examine whether the metabolic rate was decreased in synaptotagmin-7 mutant mice. NAD(P)H autofluorescence responses to 20 mM glucose were compared in mutant and control islets with regard to the timing of response, relative fluorescence increase from the basal level, and the rate of fluorescence increase. These parameters were the same in mutant and control islets: 23 ± 4 vs. 21 ± 5 s for lag time, 25 ± 5 vs. 25 ± 4 for relative fluorescence increase (in %), and 0.15 ± 0.04 vs. 0.14 ± 0.05 for the rate of increase (min^{-1}) (control vs. mutant, $n = 17$). As shown in Fig. 4*A*, the pattern of changes was also similar. Together, these data indicate that mitochondrial and glycolytic function, a key determinant of downstream secondary signals, such as $[Ca^{2+}]_i$ rise, was normal in mutant β-cells.

We then tested whether an impaired cytoplasmic calcium response was responsible for the reduced insulin secretion in mutant mice. We recorded calcium changes from Fluo-4 loaded mutant and control mouse islets that were stimulated with 10 or 20 mM glucose for 30 min. A typical cytoplasmic calcium response in pancreatic islets consists of a short silent period, initial lowering in $[Ca^{2+}]_i$ followed by a sharp rise and subsequent decrease. After that, the dynamics of $[Ca^{2+}]_i$ changes normally follows an oscillatory pattern (37). When stimulated with 20 mM glucose, fluorescence increases (peak amplitude) were the same in mutant and control mouse islets (101 ± 6% vs. 96 ± 6%, $n = 20$ and 21, respectively). There was no difference in lag time (104 ± 6 s vs. 106 ± 7 s), or nadir of initial lowering (25 ± 2% vs. 22 ± 3%, mutant vs. control). The rate of calcium oscillations during the last 25 min of the recording after the first peak was similar in mutant and control mouse islets (0.2 ± 0.02 min^{-1} and 0.2 ± 0.02 min^{-1}, $n = 5$ mutant, 4 control). To better resolve $[Ca^{2+}]_i$ oscillations, we recorded responses from islets stimulated with 10 mM glucose to obtain the oscillatory pattern of calcium changes from a larger number of islets with a higher amplitude (37). There was no difference in oscillation rate between mutant (0.42 ± 0.04 min^{-1}) and control islets ($0.33 \pm$

Table 1. Physiological characterization of body composition, glucose and insulin levels, and ultrastructural analysis of Syt7$^{-/-}$ and control mice

	Control mice		Syt7$^{-/-}$ mice		
Characteristic	Mean ± SEM	No.	Mean ± SEM	No.	Statistics
Body weight, g	30 ± 0.5	41	27 ± 0.5	44	$P < 0.001$
Body fat, %	11.3 ± 0.7	9	7.6 ± 0.6	13	$P < 0.001$
Body lean, %	74.9 ± 0.7	9	78.3 ± 0.6	13	NS
Fasting glucose, mmol/liter	6.2 ± 0.4	13	6.2 ± 0.3	17	NS
Resting glucose, mmol/liter	8.3 ± 0.4	17	8.4 ± 0.3	17	NS
Fasting insulin, ng/ml	0.27 ± 0.07	14	0.16 ± 0.03	16	$P < 0.05$
Resting insulin, ng/ml	1.02 ± 0.16	12	0.74 ± 0.14	15	NS
Islet area (×1,000 μm^2)	16.6 ± 4.9	36	17.4 ± 2.8	26	NS
Cell number per 100 μm^2 of islet area	55 ± 3	23	53 ± 2	25	NS

NS, not significant.

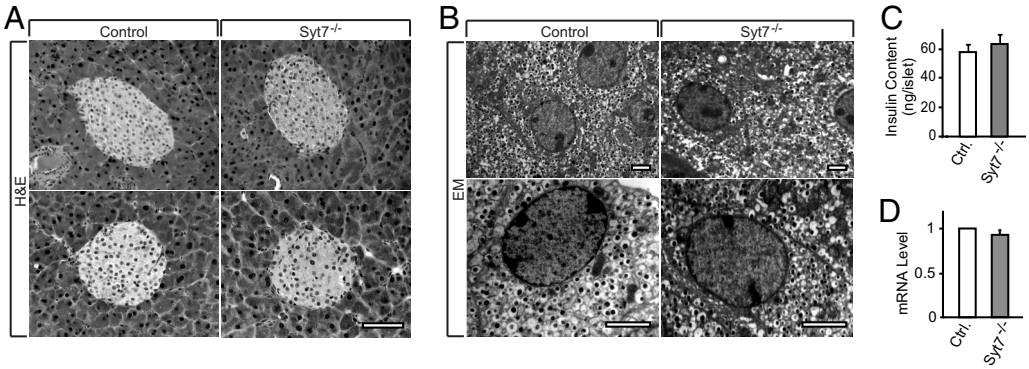

Fig. 3. Normal islet architecture, ultrastructural organizations, and insulin production in synaptotagmin-7 mutant mice. (*A*) Islet architecture and size were analyzed by using histological sections stained with hematoxylin and eosin (H&E). Two representative sections are shown for both mutant and control islets. Gross architecture and size of mutant mouse islets were not different from those of the control. (Scale bar, 50 μm.) (*B*) Ultrastructure of β-cells was analyzed by transmission EM. Two representative images from each genotype (mutant and control) are shown. Ultrastructural organizations, including distribution and number of insulin-containing secretory granules, were similar in control and mutant mouse β-cells. (Scale bars: 2 μm.) (*C*) Insulin contents were measured in isolated individual pancreatic islets from synaptotagmin-7 mutant (Syt7$^{-/-}$) and control mice, using ELISA. Isolated islets were incubated at 3 mM glucose for 2 h before they were lysed by sonication. Data are presented as means ± SEM. $n = 19$ for control and 14 for mutant. (*D*) Insulin mRNA levels were analyzed by real time PCR from total RNA extracted from isolated islets. Insulin mRNA level was not altered based on two separate qPCR experiments from pooled islets of three to five mutant or control mice.

0.03 min^{-1}) ($n = 9$). The above data demonstrate that mutant mice produce normal cytoplasmic calcium responses upon glucose stimulation and indicate that the defect responsible for the reduced insulin secretion lies downstream of the Ca^{2+} signal.

Impaired Glucose-Induced Insulin Release in Synaptotagmin-7 Mutant Mouse Islets *in Vitro*. To determine the time course of glucose-induced insulin secretion in control and mutant mice, we first incubated batches of isolated and cultured islets in 3 mM glucose for 60 min, then perifused in 3 mM glucose for an additional 30 min at 37°C before switching perifusion to 20 mM glucose. Perifusion medium was collected every 3 min starting from 6 min before stimulation (Fig. 5*A*). There was no difference in insulin release between mutant and control mouse islets during the 6 min before the stimulation started (Fig. 5*A*). In control islets, elevation of glucose concentration from 3 to 20 mM caused ≈10-fold enhancement of secretion, which showed two peaks: The first started at the 0- to 3-min interval and reached its maximum at 6–9 min, and the second occurred at 21–24 min (Fig. 5*A*). In mutant mouse islets, the insulin secretion curve had a similar biphasic pattern; however, the first phase of insulin release was significantly reduced, and the second phase was also impaired (Fig. 5*A*). Net insulin secretion by glucose stimulation was calculated as the sum of corresponding fractions after baseline subtraction. Total amount of net insulin secretion, which was the sum of all fractions over the entire stimulation period, was lower in islets from mutant mice than from controls (Fig. 5*B*). Net insulin secretion during the first 15 min of stimulation, corresponding to the first phase, was reduced by >40% in mutant islets compared with controls (Fig. 5*B*). When analyzed in islets from female mice, glucose-stimulated insulin secretion during the first phase and during the entire stimulation period was similarly affected by the synaptotagmin-7 deletion as found in male mice (SI Fig. 9).

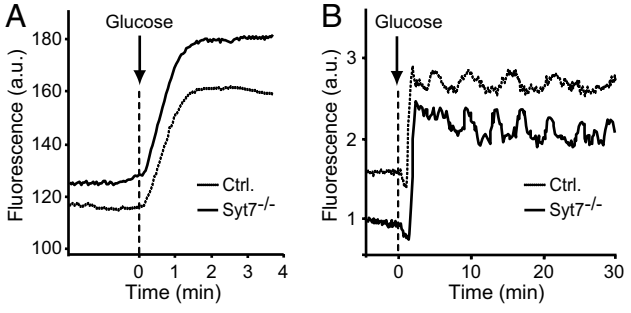

Fig. 4. Glucose metabolism and Ca^{2+} response are unaffected in synaptotagmin-7 mutant mouse islets. (*A*) Representative traces of NADH autofluorescence from synaptotagmin-7 mutant (Syt7$^{-/-}$, solid line) and control (dotted line) mouse islets perifused with 20 mM glucose ($n = 14$ for each group). Both synaptotagmin-7 mutant and control displayed similar time course and extent of autofluorescence change. Rise over basal level (%) and rate of rise are presented in *Results*. (*B*) Representative Ca^{2+} responses to 20 mM glucose from a control (dotted line) and a mutant (solid line) mouse islet ($n = 20$ control, $n = 21$ Syt7$^{-/-}$). Cytosolic $[Ca^{2+}]_i$ was measured by using Ca^{2+} indicator Fluo-4. Glucose-induced Ca^{2+} changes were similar in control and mutant mouse with regard to lag time, rise, initial lowering and oscillations. Refer to *Results* for mean values of lag time for $[Ca^{2+}]_i$ rise, rise over basal (%), initial lowering nadir, and oscillation rate. Data are presented as fluorescence intensity in arbitrary units.

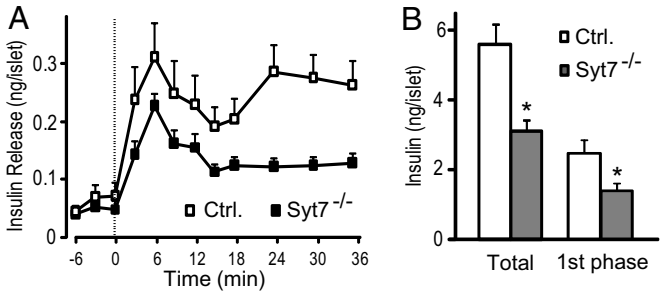

Fig. 5. Stimulated insulin secretion is reduced in isolated synaptotagmin-7 mutant mouse islets. (*A*) Glucose-induced insulin secretion from isolated islets was measured in perifusion experiments at a glucose concentration of 3 mM (basal) or 20 mM (stimulatory). The perfusate was collected in 3-min intervals, and insulin levels were determined by using ELISA. Synaptotagmin-7 mutant islets (Syt7$^{-/-}$, filled square) displayed impaired insulin secretion when compared with control (open square). (*B*) Glucose-induced insulin secretion for the entire stimulation period (Total) or the first phase (during the first 15 min after stimulation) in the perifusion experiments was lower in isolated islets from mutant (gray bar) than from control (white bar). Insulin secretion was calculated by integrating the area under each curve in *A* after baseline subtraction. Data are presented as mean ± SEM. $n = 9$ for mutant and 10 for control. *, $P < 0.05$.

Discussion

At least 15 synaptotagmin isoforms have been identified in brain and peripheral tissues (24, 25), but only synaptotagmin-1, -2, and -9 have an established function as Ca^{2+} sensors for fast neurotransmitter release (16–22). How these synaptotagmins perform their function in regulating the final steps of synaptic vesicle exocytosis has begun to emerge in recent studies (38–40). Based on previous genetic and structural studies, synaptotagmin-1 was proposed to trigger fast synchronous neurotransmitter release upon Ca^{2+} influx by binding to SNARE complexes, displacing complexin, and coupling the SNARE complex to phospholipids (38). Although other synaptotagmins have been characterized in terms of their Ca^{2+}-dependent binding properties to phospholipids and to SNARE proteins (24, 29, 31, 32, 41), none has been assigned a definitive function. Because all synaptotagmins share a common domain structure, and like synaptotagmin-1, some members bind to phospholipids and syntaxin in a Ca^{2+}-dependent manner, their wide distribution in brain and neuroendocrine systems has prompted a hypothesis for their functions as Ca^{2+} sensors for other vesicle trafficking events, modeled after a synaptotagmin-1 paradigm (24, 29, 41). Similar to synaptic vesicle exocytosis and neurotransmitter release, exocytosis of insulin-containing secretory granules may also be regulated by more than one Ca^{2+} sensor with different affinities (30). Among these other synaptotagmins, synaptotagmin-7 is one of the most abundant (24), and its C_2-domains have a 10- to 20-fold higher Ca^{2+} affinity than those of synaptotagmin-1 and -2 (29). Furthermore, synaptotagmin-7, along with several other synaptotagmins, has been shown to be present and to regulate insulin secretion in several insulin-secreting cell lines (10, 11, 13).

Given that synaptotagmin-7 binds to Ca^{2+} at micromolar level and that it is localized to β-cells (10), consistent with its function as a high-affinity Ca^{2+} sensor for insulin release, we tested this hypothesis in a mouse strain that has no detectable synaptotagmin-7 protein. Generation of the mice was described by Maximov *et al*. (42). The same mouse strain was also used in a separate study on the function of synaptotagmin-7 in large dense-core vesicle exocytosis in chromaffin cells (43). In the present study, the effects of synaptotagmin-7 deletion on the physiology of the whole animal and on the function of pancreatic β-cells *in vivo* are shown. We report that, when compared with control, synaptotagmin-7 mutant mice have reduced insulin secretion and consequentially impaired glucose tolerance. Although the amount of secreted insulin in response to glucose challenge is lower than that of controls, these mice do not become hyperglycaemic in their fed or fasted state. However, their fasting insulin levels are lower, and their blood glucose levels stay elevated longer than controls after glucose injection during IPGTT. This correlates, as expected, with lower plasma insulin levels during the glucose tolerance test.

As the major anabolic hormone in the body, insulin promotes lipid synthesis and inhibits lipolysis, in addition to lowering blood glucose levels. In agreement with a lower plasma insulin level, body fat content was slightly but significantly lower in synaptotagmin-7 mutant mice. Body fat contents are inversely correlated with animals' glucose clearance ability, i.e., animals with lower body fat contents may have higher sensitivity to insulin. Indeed, exogenous insulin administration suppresses plasma glucose more effectively in synaptotagmin-7 mutant mice than in controls, as shown in ITT. This provides a ready explanation why mutant animals do not develop hyperglycaemia in early age (14–16 weeks old); that is, they have a higher sensitivity to insulin, and even a lower level of insulin may be sufficient to maintain blood glucose homeostasis under usual conditions. Because insulin inhibits endogenous glucose production by the liver in the fasting state, the normal fasting glucose levels in mutant mice suggest that hepatorenal insulin sensitivity is not affected in these mice.

Synaptotagmin-7 mutant mice exhibited some characteristics resembling prediabetic conditions in humans, such as glucose intolerance and impaired insulin release. However, in contrast to diabetic patients, whose insulin secretion fails to meet body's needs to overcome insulin resistance, synaptotagmin-7 mutant mice have lower insulin levels from birth, and they may have adapted to this by becoming more sensitive to insulin; for example, our initial analysis showed that liver insulin receptor mRNA was up-regulated in mutant mice.

The glucose intolerance in synaptotagmin-7 mutant mice did not appear to be caused by peripheral insulin resistance, but rather by insulin secretory dysfunction in β-cells. This notion was further supported by glucose-induced insulin secretion measurements in isolated islet perifusion experiments: Both the first phase and total insulin secretion were decreased in mutant mice compared with controls. There was no difference in mRNA levels or insulin production between mutant and control mice. Islet architecture and organization, and ultrastructural analysis on insulin-containing secretory granule distribution by EM did not reveal any abnormalities. Therefore, the impaired insulin secretion likely was caused by a defect in either generating a rise in $[Ca^{2+}]_i$ or the Ca^{2+} sensor/exocytotic machinery.

In pancreatic β-cells, $[Ca^{2+}]_i$ rise is initiated by the Ca^{2+} influx through the opening of Ca^{2+} channels upon membrane depolarization caused by the closure of K_{ATP} channels under normal physiological conditions (7). K_{ATP} channels are regulated by cytoplasmic ATP/ADP ratio, a direct consequence of increased glucose metabolism. NAD(P)H autofluorescence could be used as an indirect measure to monitor the metabolic states of glycolysis and mitochondrial ATP production, because of concomitant NAD reduction by glycolysis and in the TCA cycle (36). No difference was observed in NAD(P)H autofluorescence signals in response to high glucose stimulation between mutant and control mouse islets. Glucose-stimulated cytoplasmic Ca^{2+} responses, such as the lag time, $[Ca^{2+}]_i$ rise, and oscillations, were unaffected in the presence or absence of synaptotagmin-7 protein. Thus, we can rule out all of the steps upstream of Ca^{2+} sensing during exocytosis as the cause of the secretory defect, consistent with the hypothesis that synaptotagmin-7 may be one of the calcium sensors regulating insulin secretion in pancreatic β-cells.

Although the first phase of glucose-induced insulin secretion is decreased, it is not abolished, suggesting additional protein(s) either partially substitutes synaptotagmin-7 function, or also participates in Ca^{2+} sensing in the regulation of insulin secretion. Other members of the synaptotagmin family that are expressed in insulin-secreting cells may be up-regulated and functionally compensate for decreased synaptotagmin-7.

Diabetic and insulin resistant phenotypes are usually more pronounced and readily detectable in male than in female animals (33, 34), so it was not surprising that we detected glucose intolerance in male but not female synaptotagmin-7 mutant mice in the whole-animal-level studies. To understand whether different secretory machinery components, such as Ca^{2+} sensors, were used in male and female mice, we performed *in vitro* insulin secretion measurements, using cultured islets isolated from both sexes with the assumption that such experiments preclude hormonal effects. Glucose-induced insulin secretion during the first phase and the entire stimulation period was similarly affected in islets isolated from male or female mutant mice compared with their control, indicating that the same molecular mechanisms of Ca^{2+} sensing apply to both sexes.

In summary, we showed that synaptotagmin-7 mutant mice have reduced insulin secretion and consequent glucose intolerance. The impairment of insulin secretion was likely caused by a defect in Ca^{2+} sensing in insulin-containing granule exocytosis,

because the mutant mice exhibited no abnormalities in steps leading to the rise of $[Ca^{2+}]_i$ or peripheral insulin sensitivity. These data support synaptotagmin-7 as a calcium sensor regulating insulin secretion. Furthermore, the present study emphasized the importance of insulin exocytosis mechanism in the maintenance of glucose homeostasis and protection of β cell function in the prevention of diabetic development.

Materials and Methods

Synaptotagmin-7 Mutant Mice. The synaptotagmin-7 mutant mice were generated on C57BL/6 background as described in ref. 42. Synaptotagmin-7 heterozygous mice were used for breeding to generate homozygous mutant and littermate controls. All mice used in this study were bred and housed in our animal facility. All experiments involving animals were reviewed and approved by the University of Texas Southwestern Medical Center and A*STAR Institutional Animal Care and Use Committees.

Physiology Measurements and Tests. Body composition of age-matched mutant and control littermates was measured by using an EchoMRI-100 (Echo Medical Systems). Refer to *SI Text* for detailed descriptions of physiology tests and other methods used in this study.

Histological Analysis and Electron Microscopy. Routine histological analysis and immune-labeling were performed on pancreata from four animals of each group, and EM sections were examined by using a JEOL JEM-1220 electron microscope.

Islet Isolation and Insulin, Ca^{2+}, and NAD(P)H Measurements. Islets were isolated by liberase digestion and cultured for 24 h at 11.1 mM glucose in hCell medium. Subsequent experimental handling was performed with Krebs-Ringer medium supplemented with 1 mg/ml BSA, 3 mM D-glucose, and 20 mM Hepes (pH 7.4). Islet insulin content was estimated by ELISA (Mercodia) after islets were lysed by sonication. Ca^{2+} and NAD(P)H measurements were performed on isolated and cultured islets, using a Zeiss confocal microscope equipped with an Axiocam cooled CCD camera.

Statistical Analysis. The data are presented as means ± SEM. Comparisons of data were made by using two-tailed Student's *t* test. The significance limit was set at $P < 0.05$.

ACKNOWLEDGMENTS. We thank Dr. Britton Chance for helping set up NAD(P)H measurement and for many insightful discussions and guidance; Cynthia Teo, Jian'er Lin, Andrea Roth and Nicky Hamlin for excellent technical support; and Candy Zhuang and Xiao Yong for assistance with confocal microscope. This work was supported by the Biomedical Research Council of A*STAR (Agency for Science, Technology, and Research), Singapore (G.K.R. and W.H.) and an American Diabetes Association Research Award (to J.J.R.).

1. Porte D, Jr (1991) Banting lecture 1990. Beta-cells in type II diabetes mellitus. *Diabetes* 40:166–180.
2. Ashcroft FM, Rorsman P (2004) Molecular defects in insulin secretion in type-2 diabetes. *Rev Endocr Metab Disord* 5:135–142.
3. Henquin, J.-C., *et al.* (2002) Signals and Pools Underlying Biphasic Insulin Secretion. *Diabetes* 51:S60–S67.
4. Rorsman P, Renstrom E (2003) Insulin granule dynamics in pancreatic beta cells. *Diabetologia* 46:1029–1045.
5. Kahn SE, *et al.* (2001) Importance of early phase insulin secretion to intravenous glucose tolerance in subjects with type 2 diabetes mellitus. *J Clin Endocrinol Metab* 86:5824–5829.
6. Hosker JP, *et al.* (1989) Similar reduction of first- and second-phase B-cell responses at three different glucose levels in type II diabetes and the effect of gliclazide therapy. *Metabolism* 38:767–772.
7. Ashcroft FM, *et al.* (1994) Stimulus-secretion coupling in pancreatic beta cells. *J Cell Biochem* 55(Suppl):54–65.
8. Jahn R, Südhof TC (1999) Membrane fusion and exocytosis. *Annu Rev Biochem* 68:863–911.
9. Gerber SH, Südhof TC (2002) Molecular determinants of regulated exocytosis. *Diabetes* 51(Suppl 1):S3–S11.
10. Gao Z, *et al.* (2000) Synaptotagmin III/VII isoforms mediate Ca^{2+}-induced insulin secretion in pancreatic islet beta -cells. *J Biol Chem* 275:36079–36085.
11. Iezzi M, Eliasson L, Fukuda M, Wollheim CB (2005) Adenovirus-mediated silencing of synaptotagmin 9 inhibits Ca^{2+}-dependent insulin secretion in islets. *FEBS Lett* 579:5241–5246.
12. Mizuta M, *et al.* (1997) Localization and functional role of synaptotagmin III in insulin secretory vesicles in pancreatic beta-cells. *Diabetes* 46:2002–2006.
13. Iezzi M, Kouri G, Fukuda M, Wollheim CB (2004) Synaptotagmin V, IX isoforms control Ca^{2+} -dependent insulin exocytosis. *J Cell Sci* 117:3119–3127.
14. Brown H, *et al.* (2000) Synaptotagmin III isoform is compartmentalized in pancreatic beta-cells and has a functional role in exocytosis. *Diabetes* 49:383–391.
15. Gauthier BR, *et al.* (2007) Synaptotagmin VII splice variants {alpha}, {beta}, and {delta} are expressed in pancreatic {beta}-cells and regulate insulin exocytosis. *FASEB J* 22(1):194–206.
16. Broadie K, *et al.* (1994) Absence of synaptotagmin disrupts excitation-secretion coupling during synaptic transmission. *Proc Natl Acad Sci USA* 91:10727–10731.
17. Fernandez-Chacon R, *et al.* (2001) Synaptotagmin I functions as a calcium regulator of release probability. *Nature* 410:41–49.
18. Geppert M, *et al.* (1994) Synaptotagmin I: a major Ca^{2+} sensor for transmitter release at a central synapse. *Cell* 79:717–727.
19. Pang ZP, *et al.* (2006) Genetic analysis of synaptotagmin 2 in spontaneous and Ca^{2+}-triggered neurotransmitter release. *EMBO J* 25:2039–2050.
20. Littleton JT, *et al.* (1993) Mutational analysis of *Drosophila* synaptotagmin demonstrates its essential role in Ca^{2+}-activated neurotransmitter release. *Cell* 74:1125–1134.
21. Nonet ML, Grundahl K, Meyer BJ, Rand JB (1993) Synaptic function is impaired but not eliminated in *C. elegans* mutants lacking synaptotagmin. *Cell* 73:1291–1305.
22. Xu J, Mashimo T, Südhof TC (2007) Synaptotagmin-1, -2, and -9: Ca^{2+} sensors for fast release that specify distinct presynaptic properties in subsets of neurons. *Neuron* 54:567–581.
23. Shoji-Kasai Y, *et al.* (1992) Neurotransmitter release from synaptotagmin-deficient clonal variants of PC12 cells. *Science* 256:1821–1823.
24. Südhof TC (2002) Synaptotagmins: why so many? *J Biol Chem* 277:7629–7632.
25. Craxton M (2001) Genomic analysis of synaptotagmin genes. *Genomics* 77:43–49.
26. Rizo J, Südhof TC (1998) C2-domains, structure and function of a universal Ca^{2+}-binding domain. *J Biol Chem* 273:15879–15882.
27. Sugita S, *et al.* (2001) Synaptotagmin VII as a plasma membrane Ca^{2+} sensor in exocytosis. *Neuron* 30:459–473.
28. Lynch KL, Martin TF (2007) Synaptotagmins I, IX function redundantly in regulated exocytosis but not endocytosis in PC12 cells. *J Cell Sci* 120:617–627.
29. Sugita S, *et al.* (2002) Synaptotagmins form a hierarchy of exocytotic Ca^{2+} sensors with distinct Ca^{2+} affinities. *EMBO J* 21:270–280.
30. Barg S, Rorsman P (2004) Insulin secretion: A high-affinity Ca^{2+} sensor after all? *J Gen Physiol* 124:623–625.
31. Li C, Davletov BA, Südhof TC (1995) Distinct Ca^{2+} and Sr^{2+} binding properties of synaptotagmins. Definition of candidate Ca^{2+} sensors for the fast and slow components of neurotransmitter release. *J Biol Chem* 270:24898–24902.
32. Li C, *et al.* (1995) Ca^{2+}-dependent and -independent activities of neural and non-neural synaptotagmins. *Nature* 375:594–599.
33. Kido Y, *et al.* (2000) Tissue-specific insulin resistance in mice with mutations in the insulin receptor, IRS-1, and IRS-2. *J Clin Invest* 105:199–205.
34. Yaekura K, *et al.* (2003) Insulin secretory deficiency and glucose intolerance in Rab3A null mice. *J Biol Chem* 278:9715–9721.
35. Boden G, *et al.* (1994) Mechanisms of fatty acid-induced inhibition of glucose uptake. *J Clin Invest* 93:2438–2446.
36. Bennett BD, *et al.* (1996) Quantitative subcellular imaging of glucose metabolism within intact pancreatic islets. *J Biol Chem* 271:3647–3651.
37. Bergsten P (1998) Glucose-induced pulsatile insulin release from single islets at stable and oscillatory cytoplasmic Ca^{2+}. *Am J Physiol* 274:E796–E800.
38. Tang J, *et al.* (2006) A complexin/synaptotagmin 1 switch controls fast synaptic vesicle exocytosis. *Cell* 126:1175–1187.
39. Giraudo CG, Eng WS, Melia TJ, Rothman JE (2006) A clamping mechanism involved in SNARE-dependent exocytosis. *Science* 313:676–680.
40. Bhalla A, Chicka MC, Tucker WC, Chapman ER (2006) Ca^{2+}-synaptotagmin directly regulates t-SNARE function during reconstituted membrane fusion. *Nat Struct Mol Biol* 13:323–330.
41. Hui E, *et al.* (2005) Three distinct kinetic groupings of the synaptotagmin family: Candidate sensors for rapid and delayed exocytosis. *Proc Natl Acad Sci USA* 102:5210–5214.
42. Maximov A, *et al.* (2008) Genetic analysis of synaptotagmin-7 function in synaptic vesicle exocytosis. *Proc Natl Acad Sci* 105:3986–3991.
43. Schonn J-S, *et al.* (2008) Synaptotagmin-1 and -7 are functionally overlapping Ca^{2+} sensors for exocytosis in adrenal chromaffin cells. *Proc Natl Acad Sci* 105:3998–4003.